

Angular dependence of proton-induced single event transient in silicon-germanium heterojunction bipolar transistors

Jianan Wei(魏佳男), Yang Li(李洋), Wenlong Liao(廖文龙), Fang Liu(刘方), Yonghong Li(李永宏), Jiancheng Liu(刘建成), Chaohui He(贺朝会), and Gang Guo(郭刚)

Citation: Chin. Phys. B, 2022, 31 (**8**): 086106. DOI: 10.1088/1674-1056/ac5d32
Journal homepage: http://cpb.iphy.ac.cn; http://iopscience.iop.org/cpb

What follows is a list of articles you may be interested in

Impact of proton-induced alteration of carrier lifetime on single-event transient in SiGe heterojunction bipolar transistor

Jia-Nan Wei(魏佳男), Chao-Hui He(贺朝会), Pei Li(李培), Yong-Hong Li(李永宏), Hong-Xia Guo(郭红霞)
Chin. Phys. B, 2019, 28 (**7**): 076106. DOI: 10.1088/1674-1056/28/7/076106

Mechanism of floating body effect mitigation via cutting off source injection in a fully-depleted silicon-on-insulator technology

Pengcheng Huang(黄鹏程), Shuming Chen(陈书明), Jianjun Chen(陈建军)
Chin. Phys. B, 2016, 25 (**3**): 036103. DOI: 10.1088/1674-1056/25/3/036103

Comparison of total dose effects on SiGe heterojunction bipolar transistors induced by different swift heavy ion irradiation

Sun Ya-Bin, Fu Jun, Xu Jun, Wang Yu-Dong, Zhou Wei, Zhang Wei, Cui Jie, Li Gao-Qing, Liu Zhi-Hong
Chin. Phys. B, 2014, 23 (**11**): 116104. DOI: 10.1088/1674-1056/23/11/116104

A single-event transient induced by a pulsed laser in a silicon-germanium heterojunction bipolar transistor

Sun Ya-Bin, Fu Jun, Xu Jun, Wang Yu-Dong, Zhou Wei, Zhang Wei, Cui Jie, Li Gao-Qing, Liu Zhi-Hong, Yu Yong-Tao, Ma Ying-Qi, Feng Guo-Qiang, Han Jian-Wei
Chin. Phys. B, 2013, 22 (**5**): 056103. DOI: 10.1088/1674-1056/22/5/056103

Dual role of multiple-transistor charge sharing collection in single-event transient

Guo Yang, Chen Jian-Jun, He Yi-Bai, Liang Bin, Liu Bi-Wei
Chin. Phys. B, 2013, 22 (**4**): 046103. DOI: 10.1088/1674-1056/22/4/046103

Angular dependence of proton-induced single event transient in silicon-germanium heterojunction bipolar transistors

Jianan Wei(魏佳男)[1,2,†], Yang Li(李洋)[2], Wenlong Liao(廖文龙)[2], Fang Liu(刘方)[2], Yonghong Li(李永宏)[2], Jiancheng Liu(刘建成)[3], Chaohui He(贺朝会)[2], and Gang Guo(郭刚)[3]

[1] *Science and Technology on Analog Integrated Circuit Laboratory, Chongqing* 400060, *China*
[2] *School of Nuclear Science and technology, Xi'an Jiaotong University, Xi'an* 710049, *China*
[3] *National Innovation Center of Radiation Application, China Institute of Atomic Energy, Beijing* 102413, *China*

(Received 31 December 2021; revised manuscript received 8 March 2022; accepted manuscript online 14 March 2022)

We investigate the angular dependence of proton-induced single event transient (SET) in silicon-germanium heterojunction bipolar transistors. Experimental results show that the overall SET cross section is almost independent of proton incident angle. However, the proportion of SET events with long duration and high integral charge collection grows significantly with the increasing angle. Monte Carlo simulations demonstrate that the integral cross section of proton incident events with high ionizing energy deposition in the sensitive volume tends to be higher at larger incident angles, which is associated with the angular distribution of proton-induced secondary particles and the geometry of sensitive volume.

Keywords: heterojunction bipolar transistor, proton irradiation, single event transient, angular effect

PACS: 61.80.Ed, 61.80.Jh, 85.50.Gk **DOI:** 10.1088/1674-1056/ac5d32

1. Introduction

Silicon-germanium heterojunction bipolar transistors (SiGe HBTs) are favored for space applications due to the superior low-temperature performance and the better tolerance to total ionizing dose and displacement damage than traditional silicon bipolar junction transistors (Si BJTs).[1–6] The silicon-based bandgap engineering provides a way to combine Ⅲ–Ⅴ performance with the yield and cost advantages of bulk silicon into an ideal platform.[7,8] However, SiGe HBTs are confirmed to be very sensitive to single event effect (SEE).[9–11] Integrated circuits (ICs) based on SiGe HBT and SiGe BiCMOS technologies usually suffer from low SEE thresholds and large SEE cross sections.[12–14] Therefore, the detailed characteristics of single event transient (SET) in SiGe HBTs are important for a full understanding of behavior of SiGe ICs in particular radiation environments.

Heavy ions and protons are the two dominant causes for SEE in spaceborne electronics. Some previous publications have investigated the current transients induced by heavy ions in SiGe HBTs via experiments and technology computer aided design (TCAD) simulations.[11,15–18] The results indicate that the large-area collector–substrate junction and the lightly doped substrate are the two dominant factors for the collection of excess carriers generated by incident ions. However, the SET induced by protons in SiGe HBTs is rarely investigated from a transistor level of view. In submicron semiconductor devices, protons cause SEE mainly via the secondary particles created by interactions with target materials. This is quite different from heavy ions which cause SEE mainly via direct ionizing processes. The randomness of the location of proton/material interactions and the characteristics of secondary particles makes the analysis of proton-induced SET in SiGe HBTs rather complicated.[19] In our previous study,[20] we presented primary results of proton-induced SET in SiGe HBTs. The temporal information of the current transients induced by protons with energy ranging from 30 MeV to 90 MeV was measured via experiment for the first time. However, the incident angle of protons was fixed at 0° (normal to the device surface), so that the impact of incident angle of protons was not discussed at that time. Note that protons from the radiation belts can penetrate low altitude orbiting spacecrafts from all directions, it is still essential to make further supplements.

In this work, we present the first investigation into the angular dependence of proton-induced SET in SiGe HBTs. The collector transient currents induced by 60 MeV protons at different incident angles are measured. Then the angular effect on the current transient duration and integral charge collection are discussed. Furthermore, the ionizing energy deposition in the sensitive volume and the angular distribution of proton-induced secondary particles are simulated by using GEANT4 Monte Carlo toolkits in order to gain deeper insights into the underlying mechanisms.

2. Experimental setup

2.1. Device description

The devices under test (DUTs) are vertical double polysilicon NPN SiGe HBTs fabricated by a system purchased from a

†Corresponding author. E-mail: weijianan93@163.com
© 2022 Chinese Physical Society and IOP Publishing Ltd

HUAJIE company and achieve a peak h_{FE} of 150, a peak f_T of 25 GHz and a maximum collector current (I_C) of 30 mA. Figure 1 shows the schematic device structure. Figure 2 shows a localized SEM picture of the emitter-base-collector stack. The width of the emitter window is about 0.4 μm and the thickness of EB spacer is about 16 nm. The intrinsic base is formed by an epitaxially grown SiGe layer with thickness of about 100 nm. The isolation layer between collector and base is formed by local oxidation of silicon (LOCOS) with a thickness of about 675 nm. More detailed information about the DUTs can be found in Refs. [21–23].

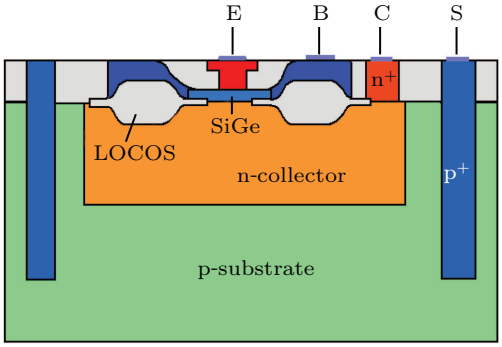


Fig. 1. Schematic cross section of the SiGe HBT (not to scale).

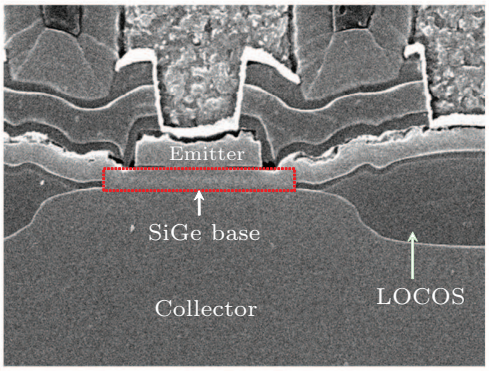


Fig. 2. SEM picture of the emitter-base-collector stack.

3. Proton irradiation

The proton irradiation experiment was carried out at the SEE testing facility of the proton cyclotron in China Institute of Atomic Energy (CIAE), Beijing, China. Figure 3 shows the components of the facility. The energy of protons is adjusted by aluminum degraders with variable thickness, while the beam spot size is adjusted by the collimator. The dosimetry measurements use a secondary-electron emission monitor calibrated against a Faraday cup. In this work, the proton energy was adjusted to 60 MeV and the spot size of proton beam was fixed at 5×5 cm^2. The flux varied from 1×10^7 cm^{-2}·s^{-1} to 2×10^7 cm^{-2}·s^{-1}, depending on the beam intensity. The incident angle of protons was controlled by the sample rack which can rotate around its central axis, as shown in Fig. 3(b), where 0° corresponds to the proton beam being incident normal to the device surface. The maximum available incident angle of the facility is 70°. Three irradiations were carried out with proton incident angles set at 0°, 30° and 60°.

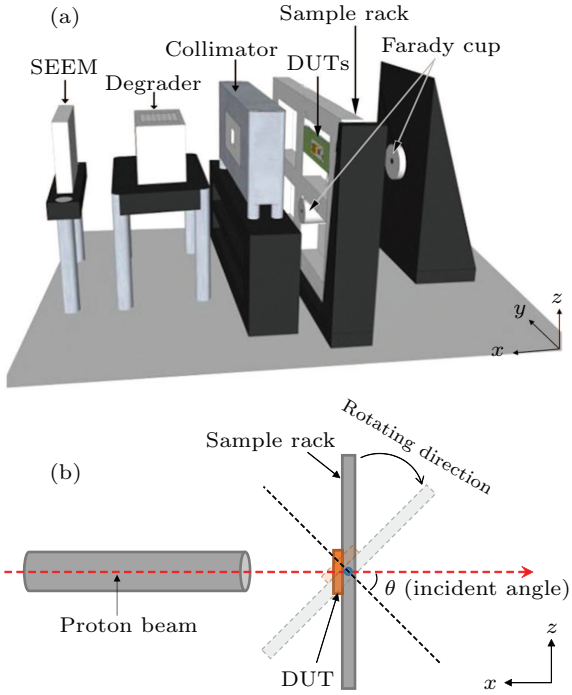


Fig. 3. Schematic of the proton SEE testing facility at CIAE.

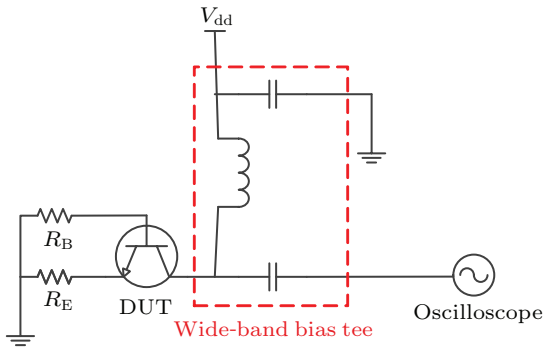


Fig. 4. Configuration of the SET testing circuit.

The external circuit components and lumped elements for SET testing are shown in Fig. 4. The proton-induced current transients on collector, which is the main cause for SEE in most SiGe circuits,[24] is recorded through a Mini-Circuits (company) wide-band bias tee by a Tektronix DPO71604 16-GHz (50 GS/s) real time digital phosphor oscilloscope. The DUTs were biased with $V_E = V_B = V_S = 0$ V and $V_C = 5$ V during irradiation. Under this condition, the collector–substrate junction is reverse-biased so that excess carriers generated by charged particles in the lightly doped substrate can be collected rapidly. This has been confirmed to be the worst case for SET. The trigger threshold was set to $|I_C| = 0.08$ mA. Three independent DUTs were tested at each proton incident angle and the total accumulated proton fluence at each angle exceeded 1.5×10^{11} cm^{-2}, which resulted in no less than 35 SET events.

4. Experimental results

Figure 5 shows the SET cross section (σ_{SET}) as a function of incident angle. The cross section is calculated by

$$\sigma_{SET} = N_{SET}/(\Phi_P \cdot \cos\theta), \quad (1)$$

where N_{SET} is the number SET events recorded by the oscilloscope, Φ_P is the proton fluence. The error bars represent the standard deviation of data from three independent DUTs. The error bar is not given for the data at 60° because function failure of the testing circuit was found for one of the three DUTs during irradiation. It can be found that the SET cross section exhibits no clear trend with incident angle, indicating a negligible angular effect. Figure 6 plots typical waveforms of recorded collector current transients at different incident angles. Each panel in the figure shows the experimental results obtained from a single DUT in a single run of proton irradiation. The accumulated fluence of a single run is no less than 5×10^{10} cm^{-2}. Most current transients exhibit similar characteristics, namely a very short rise time and a relatively longer falling time. This is consistent with the previous results. However, with the increase of proton incident angle, the falling tail of some current transients turns to be much longer, thereby increasing the duration significantly. As seen in Fig. 6, all the current transients restore to the background level in about 1 ns when the incident angle is 0°, whereas the current transients may last for more than 3 ns when the incident angle increases to 60°. Figure 7 shows the proportion of current transients with different durations. A broadening of the distribution of histograms can be found at large incident angles. Moreover, the proportion of SET events with short duration decreases with increasing incident angle, whereas the proportion of SET events with long duration increases, thereby leading to a rightward shift of the histograms. A SET event with longer duration can span a greater number of clock periods and affect more data bits if the SiGe circuit works at high frequencies.[25] On the other hand, the increase of transient duration will consequently result in a greater integral charge collection which is the time integral of transient current. Evidently, as shown in Fig. 8, the distribution of SET events with certain integral charge collection values shows similar trends to that in Fig. 7. The increasing proportion of SET events with high charge collection values has more significant impact on the circuit with a high SEE critical charge (Q_C). Figure 9 shows the cross section of SET events with collector charge collection exceeding certain values of Q_C, which is calculated by

$$\sigma_Q = N_Q/(\Phi_P \cdot \cos\theta), \quad (2)$$

where N_Q is the number of SET events with collector charge collection exceeding Q_C. The proton incident angle appears to have no clear impact on σ_Q when Q_C is set to 0.05 pC and 0.1 pC, whereas a rapid increase of σ_Q with incident angle occurs when Q_C is increased to 0.15 pC.

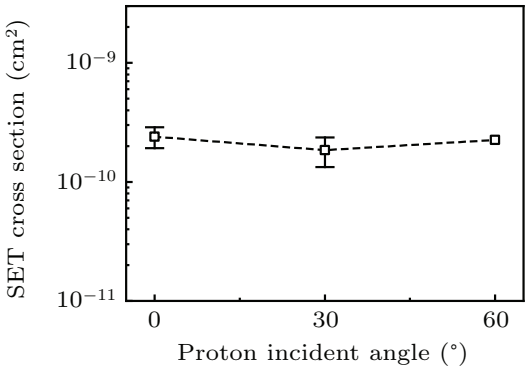


Fig. 5. SET cross section at different proton incident angles.

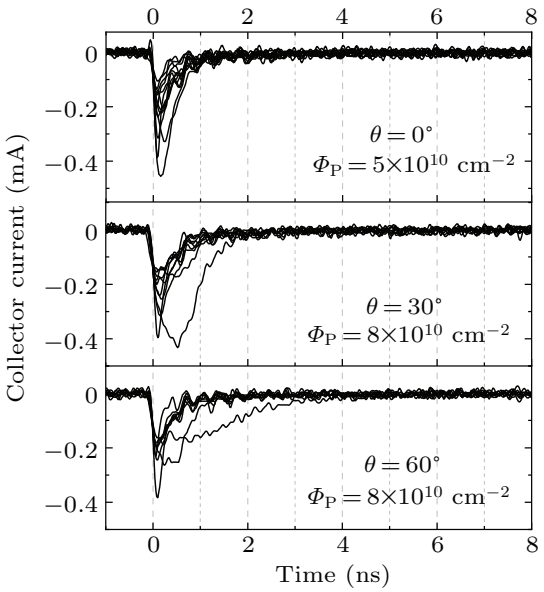


Fig. 6. Typical current transients at different proton incident angles.

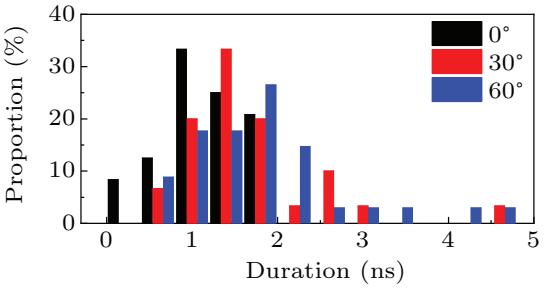


Fig. 7. Proportion of current transients with different durations.

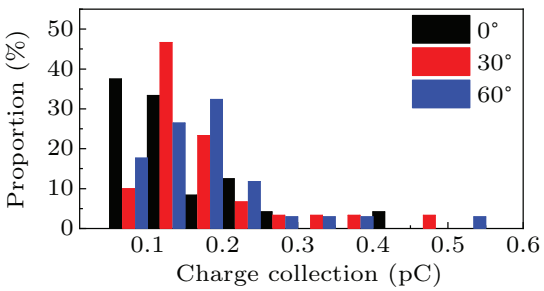


Fig. 8. Proportion of current transients with different integral charge collections.

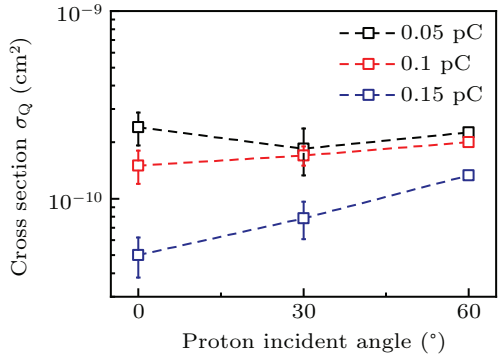


Fig. 9. Cross section of SET events with integral charge collection exceeding certain critical values.

These results suggest that the impact of proton incident angle should not be simply ignored when performing ground SET testings and the results at normal incidence may underestimate the SET susceptibility of this SiGe technology.

5. Monte Carlo simulation and discussion

In this section, the GEANT4 Monte Carlo simulation toolkits are used to better understand the mechanisms for angular dependence of proton-induced SET. In our previous work,[20] the sensitive volume geometry of this SiGe HBT has been determined based on heavy-ion microbeam irradiation and TCAD simulation results. The right rectangular parallelepiped sensitive volume has a topside area of 140×140 μm^2 and a depth of 20 μm. We use the same model configurations in this work to investigate the ionizing energy deposition in the sensitive volume and the characteristics of secondary particles at varying proton incident angles.

5.1. Ionizing energy deposition in sensitive volume

The amount of collected charge of a SET event is directly related to the ionizing energy loss in the sensitive volume. Figure 10 shows the simulated integral cross section of proton incident events that deposit a certain amount of ionizing energy or greater in the sensitive volume. It can be found that the integral cross section does not exhibit significant dependence on incident angle when the deposited ionizing energy is less than 10 MeV.

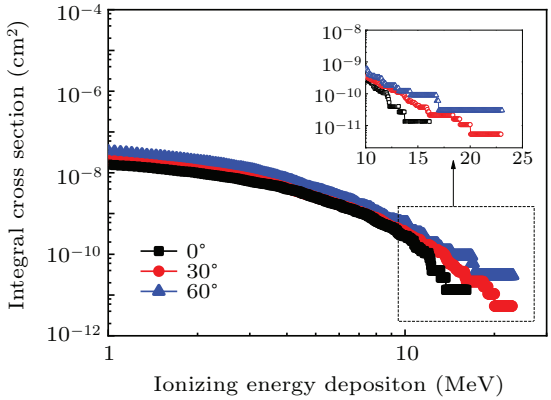


Fig. 10. Simulated integral cross section as a function of ionizing energy deposition in the sensitive volume for 60 MeV protons.

However, for the deposited energy greater than 10 MeV, the integral cross section increases significantly with the increasing incident angle, which indicates that the probability of proton incident events with large ionizing energy deposition turns to be higher at larger incident angles. This is consistent with the experimental results in Fig. 8.

5.2. Angular distribution of proton-induced secondary particles

Figure 11 shows the simulated angular distributions of proton-induced secondary particle energy, linear energy transfer (LET) and range in silicon. Information of secondary particles created through both spallation reaction and elastic nuclear scattering is collected. The launching angle is defined as the angle between the momentum directions of the secondary particles and the primary incident protons. Evidently, the secondary particles with the highest energy (highest LET, longest range) tend to have smaller launching angles, which indicates that they are forward directed. On the contrary, the secondary particles with lower energies are more isotropic, thus leading to the broader angular distributions that cover 0° to approximately 140°.

As mentioned above, the sensitive volume of the SiGe HBT is 140 μm×140 μm×20 μm, which results in an aspect ratio of 7. Under this condition, the particles that are parallel to the device surface would have longer paths than those normal to the device surface. Therefore, the forward-directed high-energy secondary particles can leave a longer ionizing track in the sensitive volume at larger proton incident angles, as shown in Fig. 12. As a consequence, the ionizing energy deposition increases since it is proportional to the track length. On the contrary, for the low-energy secondary particles that are more isotropic, the impact of incident angle becomes much smaller, as shown in Fig. 13. Therefore, the angular dependence of the proton-induced SET can be associated with the angular distribution of the secondary particles.

However, it should be emphasized that the SiGe HBTs investigated in this work were fabricated via bulk silicon technology, and the deep trench isolation (DTI) is not employed. For SiGe HBTs fabricated via silicon-on-isolator (SOI) technology, the depth of the sensitive volume is confined by the buried oxide layer,[25–27] so that a more aggressive aspect ratio can be expected, which leads to more significant angular effects. On the other hand, for the SiGe HBTs with DTI around the intrinsic device (i.e. the emitter-base-collector stack), the sensitive volume is determined by the deep trench,[11,16,28,29] which leads to an aspect ratio much smaller. Therefore, the impact of proton incident angle may vary among different SiGe technologies and should be carefully considered in the SET ground testings.

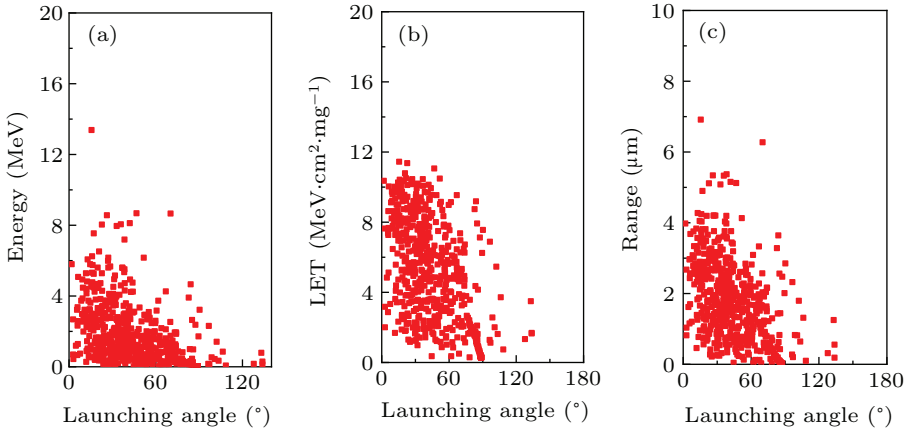


Fig. 11. Simulated angular distribution of proton-induced secondary particles: (a) energy, (b) LET, (c) range.

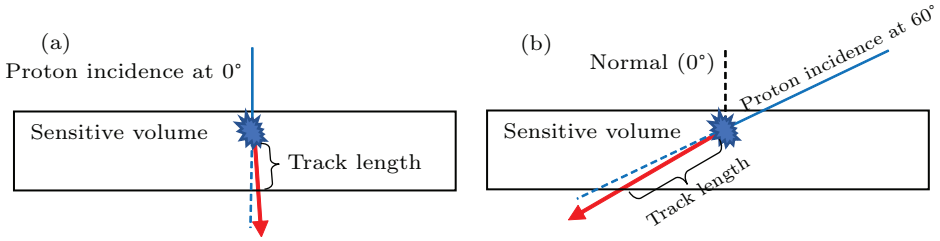


Fig. 12. Schematic of angular effect on the ionizing track length of forward-directed high-energy secondary particles in the sensitive volume: (a) proton incidence at 0°, (b) proton incidence at 60°.

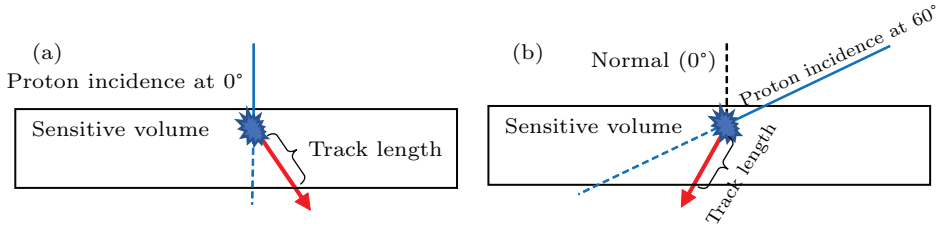


Fig. 13. Schematic of angular effect on the ionizing track length of isotropic low-energy secondary particles in the sensitive volume: (a) proton incidence at 0°, (b) proton incidence at 60°.

6. Conclusions

In summary, the angular effect of proton-induced current transient in SiGe HBT is investigated. Collector current transients caused by 60 MeV protons were measured at incident angles of 0°, 30° and 60°. The overall cross section of SET events exhibits no clear angular dependence. However, the proportion of SET events with long duration and high integral charge collection grows significantly with increasing incident angle. Monte Carlo simulation demonstrates that the integral cross section of proton incident events depositing more than 10 MeV ionizing energy in the sensitive volume grows with increasing incident angle. This can be associated with the forward-directed nature of the most energetic (highest LET, longest range) secondary particles. Given a sensitive volume with an aspect ratio of 7, the forward-directed high-energy secondary particles can leave longer ionizing tracks, thus more ionizing energy deposition and excess carriers, in the sensitive volume at larger proton incident angles.

The results of this study indicate that ground testings on SiGe devices which ignore the proton incident angle may lead to misestimations of SET susceptibility. Furthermore, the geometry of sensitive volume, which varies significantly among different SiGe technologies, must be carefully considered when assessing the angular effects of proton-induced SET.

Acknowledgements

Project supported by the National Natural Science Foundation of China (Grant Nos. 11775167 and 12105252) and the Natural Science Foundation of Chongqing, China (Grant No. cstc2021jcyj-bsh0246).

References

[1] Cressler J D 2010 *IEEE Trans. Device. Mater. Rel.* **10** 437
[2] Cressler J D 2013 *IEEE Trans. Nucl. Sci.* **60** 1992
[3] Sutton A K, Haugerud B M, Yuan L B M, *et al.* 2004 *IEEE Trans. Nucl. Sci.* **51** 3736
[4] Cressler J D 2005 *Proc. IEEE* **93** 1559
[5] Fleetwood Z E, Cardoso A S, Song I, *et al.* 2014 *IEEE Trans. Nucl. Sci.* **61** 2915
[6] Pruvost, S, Delcourt, S, Telliez, I, *et al.* 2005 *IEEE Electron Device Lett.* **26** 105

[7] Cressler J D 1998 *IEEE Trans. Microwave Theor. Technol.* **46** 572
[8] Schroter M, Rosenbaum T, Chevalier P, *et al*. 2017 *Proc. IEEE* **105** 1068
[9] Lourenco N E, Fleetwood Z E, Ildefonso A, *et al*. 2017 *IEEE Trans. Nucl. Sci.* **64** 406
[10] Montes E J, Reed R A, Pellish J A, *et al*. 2008 *IEEE Trans. Nucl. Sci.* **55** 1581
[11] Varadharajaperumal M, Guofu N, Krithivasan R, *et al*. 2004 *IEEE Trans. Nucl. Sci.* **50** 2191
[12] Marshall P W, Carts M A, Campbell A, *et al*. 2001 *IEEE Trans. Nucl. Sci.* **47** 2669
[13] Marshall, P, Carts M, Currie, S, *et al*. 2005 *IEEE Trans. Nucl. Sci.* **52** 2446
[14] Najafizadeh L, Phillips S D, Moen K A, *et al*. 2009 *IEEE Trans. Nucl. Sci.* **56** 3469
[15] Pellish J A, Reed R A, McMorrow D, *et al*. 2009 *IEEE Trans. Nucl. Sci.* **56** 3078
[16] Vizkelethy G, Phillips S D, Najafizadeh L, *et al.* 2010 *Nucl. Instrum. Methods Phys. Res. B* **268** 2092
[17] Pellish J A, Reed R A, Sutton A K, *et al*. 2007 *IEEE Trans. Nucl. Sci.* **54** 2322
[18] Wei J, He C, Li P, *et al*. 2019 *Microelectron. Reliability* **95** 28
[19] Schwank J R, Shaneyfelt M R, Baggio J, *et al*. 2006 *IEEE Trans. Nucl. Sci.* **53** 3122
[20] Wei J N, Li Y, Yang W T, *et al*. 2020 *Sci. China Technol. Sci.* **63** 851
[21] Zhang J, Guo Q, Guo H, *et al.* 2016 *IEEE Trans. Nucl. Sci.* **63** 1251
[22] Liu M H, Lu W, Ma W Y, *et al*. 2016 *Chin. Phys. C* **40** 036003
[23] Zhang J, Guo H, Zhang F, *et al*. 2017 *Sci. China Inf. Sci.* **60** 120404
[24] Reed R A, Marshall P W, Pickel J C, *et al*. 2004 *IEEE Trans. Nucl. Sci.* **50** 2184
[25] Wilcox E P, Phillips S D, Cheng P, *et al*. 2010 *IEEE Trans. Nucl. Sci.* **57** 3293
[26] Jung S, McMorrow D, Buchner S P, *et al*. 2014 *IEEE Trans. Nucl. Sci.* **61** 3193
[27] Ildefonso A, Warner J H, Cressler J D, *et al*. 2020 *IEEE Trans. Nucl. Sci.* **67** 71
[28] Wei J N, He C H, Li P, *et al*. 2019 *Chin. Phys. B* **28** 076106
[29] Pellish J A, Reed R A, Schrimpf R D, *et al*. 2006 *IEEE Trans. Nucl. Sci.* **53** 3298